Possibility of Fisher renormalization of the critical exponents in an Ising fluid

W. Fenz,[1] R. Folk,[1] I. M. Mryglod,[1,2] and I. P. Omelyan[1,2]
[1]*Institute for Theoretical Physics, Linz University, A-4040 Linz, Austria*
[2]*Institute for Condensed Matter Physics, 1 Svientsitskii Street, UA-79011 Lviv, Ukraine*
(Received 2 April 2007; published 21 June 2007)

Using Monte Carlo simulation techniques, we study the ferromagnetic order-disorder phase transition in Ising spin fluids with hard-core Yukawa interaction truncated at various cutoff radii r_c. We focus our interest on the dependence of critical quantities such as the Binder cumulant and various exponent ratios on the value of r_c, and on the question whether the Fisher-renormalized exponents expected for such systems can be observed in the simulations. It turns out that the corrections to scaling decaying with a rather small exponent prevent reaching the asymptotic region with the computational power available. Thus, we observe only effective exponents, with different (nonuniversal) values depending on the cutoff radius. The same behavior is also found for the critical Binder cumulant. Nevertheless, an exact investigation of the effective susceptibility exponent γ_{eff} as a function of temperature seems to point towards a Fisher-renormalized value. For two selected cutoff radii, the critical temperature is determined more accurately using, in addition to the cumulant crossing technique, the scanning technique and the shifting technique, taking into account corrections to scaling. Simulations of Ising fluids with constant cutoff radius and varying Yukawa-tail screening lengths λ also show a nonuniversal dependence of U_c on λ. Finally, we have performed simulations of the Ising lattice model with increasing number of couplings which show the expected asymptotic behavior, independent of the range of interactions.

DOI: 10.1103/PhysRevE.75.061504 PACS number(s): 64.60.Fr, 61.20.Ja, 75.50.Mm, 64.60.Cn

I. INTRODUCTION

The general concept of Fisher renormalization was first introduced in [1] and describes the critical properties of systems with two independent order parameters, for example, magnetization and density of impurities in a diluted Ising model. If the second (so-called hidden) variable is subject to a constraint (eg., fixed number of impurities) and the pure system has a positive specific heat exponent α, the critical exponents of the diluted system are renormalized with respect to the pure system. The originally divergent specific heat becomes finite with a new exponent $\alpha' = -\alpha/(1-\alpha)$, and all other exponents are scaled by a factor $1/(1-\alpha)$. Besides the mentioned diluted Ising model, examples for Fisher-renormalized systems are the multicomponent lattice gas [2–4] or the Blume-Capel model [5–7] for the superfluid ^{3}He-^{4}He mixture.

A class of systems that are also candidates for Fisher renormalization is the family of classical spin fluids including the Heisenberg ($n=3$), XY ($n=2$) and Ising ($n=1$) fluid, where n denotes the number of components of the spin. All of these feature both magnetization and number density as order parameters, and show gas-liquid as well as ferromagnetic order-disorder phase transitions. While in the case of the Heisenberg fluid α is negative, the Ising case has $\alpha > 0$, and thus Fisher-renormalized exponents can be expected in the canonical ensemble. The only thorough study of the critical properties of the three-dimensional Ising fluid available so far [8] reports exponents that indicate a crossover from the universal three-dimensional (3D) Ising lattice values to the Fisher-renormalized ones. In the Heisenberg case [9–11] the observed exponents also differed from those of the lattice Heisenberg model, and it was stated that these are merely effective exponents and the asymptotic critical region could not be reached since the minimum system size for corrections to scaling to become irrelevant would be of the order of $N = 10^8$, which is far beyond the particle numbers that can be studied in the present simulations. The reason for this is the small absolute value of α appearing in the exponent of the correction term, which makes the corrections decay much slower when approaching the critical temperature than the usual Wegner corrections to scaling. It is also worth mentioning that for the positionally frozen Heisenberg system [12–14], the observed critical exponents were nearly indistinguishable from those of the Heisenberg spin fluid.

In this paper we shall perform a similar study as in [9] for the Ising fluid, in order to clarify the nature of the critical exponents observed in computer simulations, using several different finite-size scaling techniques.

The second aspect we are interested in is the quantity known as the Binder cumulant U [15]. This fourth-order cumulant of the order parameter distribution has become a common tool in the field of phase transitions and critical phenomena. It is, for example, used for locating the critical point (cumulant crossing technique) or to compute the critical exponent of the correlation length. The critical value of the cumulant directly at the phase transition, U_c, has generally been considered a universal quantity that is characteristic for the universality class of the studied system. This would mean that it depends only on the dimensionality of the system and the number of components of the order parameter, but not on microscopic details such as the type of interaction or the geometric lattice structure. However, in recent years more and more studies have questioned this universality of the Binder cumulant. In [16,17], for example, the Binder cumulant is shown to be nonuniversal in a three-dimensional Ising model with isotropic nearest-neighbor coupling and anisotropic next-nearest-neighbor coupling on a simple cubic lattice.

For the class of the two-dimensional Ising model, the critical Binder cumulant has been studied extensively in numerous works [18–28], using different lattices (square, rectangular, triangular), anisotropic nearest-neighbor or next-nearest-neighbor interactions, and also different boundary conditions and lattice shapes (square, rhombus, circle) [18–23]. While the numerically determined value of U_c for spin-$\frac{1}{2}$ ferromagnetic nearest-neighbor couplings on a square lattice with periodic boundary conditions, $U_c=0.610\,69$ [19], was usually believed to be valid for the whole two-dimensional Ising universality class, it has been found to vary significantly, depending on the details of the system. Selke, for example, observed values as low as $U_c=0.379$ for a triangular lattice with rhombic shape and free boundary conditions [18]. On the other hand, for several two-dimensional systems, such as the spin-1 Ising model and even the two-dimensional anisotropic *XY* model, the estimates of U_c agree with the universal value [24–28].

Not so many studies are available to date regarding the Binder cumulant in the three-dimensional Ising model (which falls into the same universality class as the pure fluid) and the 3D Ising fluid. The former was examined in [29–32], with contradictory results concerning the nonuniversality of the susceptibility ratio in the anisotropic next-nearest-neighbor Ising model. As for the Ising fluid, where the spins are connected to particles moving freely in three-dimensional space and the exchange interaction J is a function of the particle distance, there have been several studies of the general phase behavior [33–39], both in the absence and presence of a magnetic field H. The phase diagram for $H=0$ shows, apart from the usual gas-liquid transition, a line of magnetic critical points ending either in a tricritical point or a critical endpoint, depending on the details of the interaction potential. The critical properties of this ferromagnetic order-disorder transition, however, have not received much attention so far. In Ref. [8], already mentioned earlier, they were studied for an Ising fluid with hard-core repulsion and Yukawa exchange interaction truncated at a cutoff radius $r_c=2.5\sigma$ (σ denotes the particle diameter), using both the hierarchical reference theory (HRT) [40] and Monte Carlo (MC) simulations. The critical temperature T_c was located for two reduced densities $\rho^*=\rho\sigma^3=0.3$ and $\rho^*=0.5$ with the Binder cumulant crossing technique and the values of critical exponent ratios were calculated using finite-size scaling (FSS) relations. The critical value of the Binder cumulant U_c at T_c was determined as 0.462(4) at $\rho^*=0.3$ and 0.456(6) at $\rho^*=0.5$, respectively, which was considered as consistent with the Ising lattice value 0.4652(3) [30].

An aspect that was not taken into account in that work is the influence that the choice of the cutoff radius r_c and the shape of the Yukawa function may have on the observed values of the critical Binder cumulant and the exponent ratios. In our paper, we focus on this point by looking at the same system, but choosing various values of r_c and the screening parameter λ we introduce in the Yukawa potential. We also compare the results for the Ising fluid with simulations of the 3D Ising lattice model, adding successively second-nearest and third-nearest-neighbor couplings to the nearest-neighbor interactions, thus investigating the effect of the interaction range in the lattice system.

II. ISING FLUID

We consider an Ising spin-fluid with hard-core repulsion consisting of N particles in a volume V interacting via the pair potential

$$u(r_{ij},s_i,s_j)=\begin{cases}\infty, & r_{ij}<\sigma,\\ -J(r_{ij})s_is_j, & \sigma<r_{ij}<r_c,\\ 0, & r_{ij}>r_c,\end{cases} \tag{1}$$

with a short-range Yukawa exchange interaction

$$J(r)=\varepsilon\frac{\sigma}{r}\exp[-\lambda(r-\sigma)]. \tag{2}$$

Here, σ denotes the hard-core diameter of the particles, r_c is the cutoff radius, ε is the interaction strength, λ is the Yukawa screening parameter and $r_{ij}=|\mathbf{r}_i-\mathbf{r}_j|$ the interparticle distance. The particles move in three-dimensional space at coordinates $\mathbf{r}_i=(x_i,y_i,z_i)$ and have embedded spins $s_i=\pm1$.

A. Simulations

We have conducted MC simulations in the canonical (constant-*NVT*) ensemble for Ising fluids with different cutoff radii r_c varying from 2 to 5 in steps of 0.5. The simulations were performed in a cubic box with periodic boundary conditions, at a fixed density $\rho^*=\rho\sigma^3=0.5$, with particle numbers N ranging from 108 to 10 000 (for $r_c=4$). We used standard Metropolis particle translation moves and the Wolff cluster algorithm to update the spins. Although in its original form [41] this method was formulated only for lattice systems, its application to off-lattice systems is straightforward (see, for example, Ref. [10]). Each production run consisted of at least 10^6 MC cycles, with one cycle being defined as one displacement attempt per particle followed by one Wolff update. For large system sizes, we applied the cell list method [42] in order to save computer time.

B. Binder cumulant

During a simulation with system size N at a temperature close to T_c (roughly estimated beforehand with short simulation runs), a combined histogram $H_T(m,E)$ of magnetization per particle, $m=\frac{1}{N}\Sigma_{i=1}^{N}s_i$, and the total potential energy

$$E=\sum_{i<j}^{N}u(r_{ij},s_i,s_j), \tag{3}$$

was collected, and then extrapolated to nearby temperatures using multihistogram reweighting techniques [43,44]. Thus, the canonical probability distribution of m, $P_T(m)=\Sigma_E H_T(m,E)/\Sigma_{m,E}H_T(m,E)$, was determined as a function of T, from which in turn the Binder cumulant U_N can be calculated as

$$U_N(T)=1-\frac{\langle m^4\rangle_T}{3\langle m^2\rangle_T^2}. \tag{4}$$

Here $\langle\,\rangle_T$ denotes the canonical average, $\langle f(m)\rangle_T=\int P_T(m)f(m)dm$ for some function f of m. From the func-

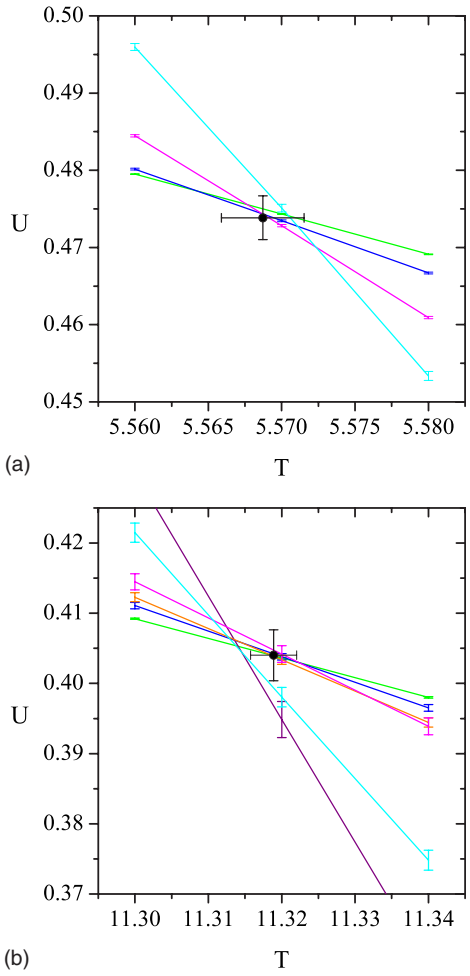

FIG. 1. (Color online) Binder cumulant $U_N(T)$ for different system sizes (N=300, 500, 1500, and 5000) of the Ising fluid with $\lambda=1$ and $r_c=2$ (a), and of the Ising fluid with $\lambda=1$ and $r_c=4$ (b) for system sizes N=300, 500, 750, 1000, 5000, and 10 000. The circles and attached error bars indicate the locations of U_c and T_c, with their corresponding uncertainties, obtained from averaging the crossing points as described in the text.

tions $U_N(T)$ for different system sizes N we determined the critical temperature T_c and critical Binder cumulant U_c as mean values of the pairwise intersection points of each two curves corresponding to consecutive system sizes (disregarding the curves for N=108, which was found to be too small of a system size for reasonable calculations without corrections to scaling). The standard deviations of the mean values were used for the error bars.

Figures 1(a) and 1(b) show the Binder cumulant functions $U_N(T)$ in the critical region for several system sizes N and two different cutoff radii $r_c=2$ and 4. The values of T_c and U_c, respectively, are indicated by the circles and the attached error bars corresponding to the standard deviations. U_c can be seen to shift from around 0.474 for $r_c=2$ to 0.404 for $r_c=4$. In Fig. 2, the dependence of the critical temperature T_c and the critical Binder cumulant U_c on the cutoff radius r_c is illustrated. All temperatures are in units ϵ/k_B with k_B being Boltzmann's constant. Error bars are displayed if they are larger than the symbol size. For the case $r_c=4$ we used larger

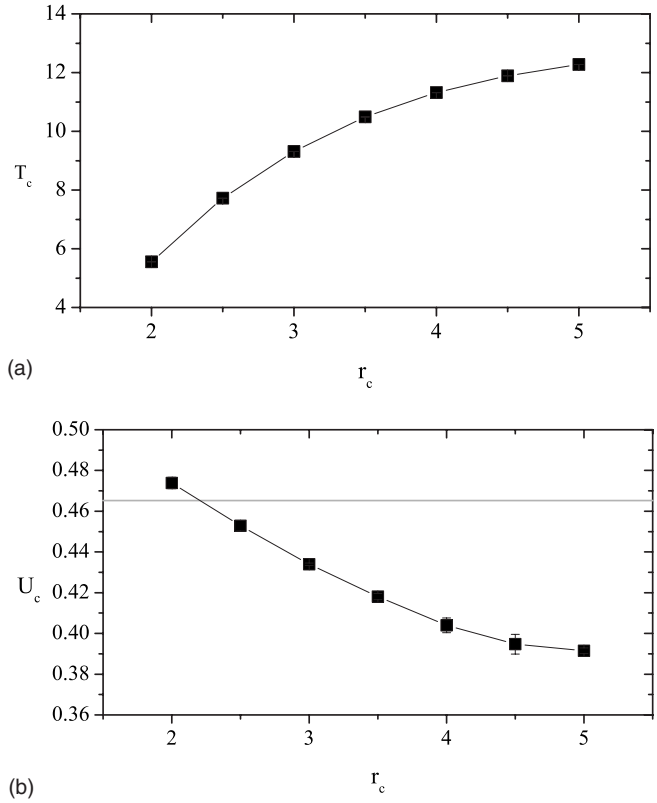

FIG. 2. Critical temperature T_c (a) and critical Binder cumulant U_c (b) of the Ising fluid with $\lambda=1$ as a function of the cutoff radius r_c. The horizontal line indicates the value of U_c for the lattice Ising model [30]. Error bars are shown if larger than the symbol size.

system sizes including N=10 000, in order to check if there is a trend towards a higher value of U_c for larger particle numbers, which would indicate that the low critical Binder cumulants we observe for higher r_c are due to finite-size effects. However, as demonstrated in Fig. 3, no sign for such

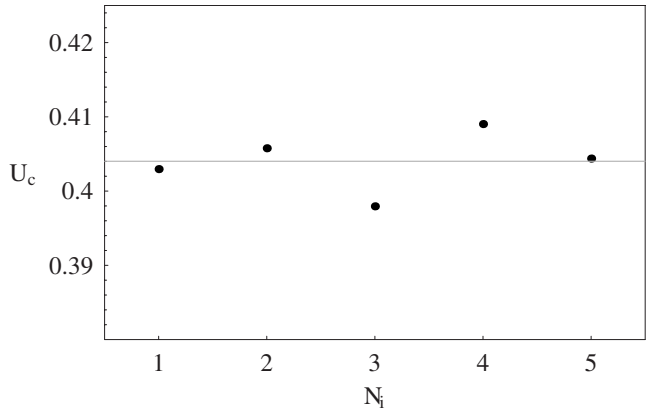

FIG. 3. Critical Binder cumulant U_c of the Ising fluid with $\lambda=1$ and cutoff radius $r_c=4$ obtained from the intersections of each two curves $U_{N_i}(T)$ and $U_{N_{i+1}}(T)$ with N_i out of the set $\{300,500,750,1000,5000,10\,000\}$ [the curves are shown in Fig. 1(b)]. The horizontal line indicates the mean value of the intersection points. No system-size dependent trend in the data can be seen.

a scenario was found within the range of system sizes accessible to our simulations.

On a side note, we have also performed some additional simulations with an interparticle potential defined as in Eq. (1), only shifted by the value at r_c, such that it goes to zero continuously. These calculations showed the same trend of the behavior of U_c in dependence on r_c, differing only quantitatively from the results we have shown.

C. Critical temperature

Apart from the cumulant crossing technique, we also applied two other methods in order to estimate more accurately the critical temperature for the cases $r_c=2.5$ and $r_c=4$. First, we used a technique that was already employed earlier for both the Heisenberg magnet [45] and fluid [9]. It is called the scanning technique and is based on six quantities V_l, $l=1,\ldots,6$, defined as

$$V_1 = 4[m^3] - 3[m^4], \tag{5}$$

$$V_2 = 2[m^2] - [m^4], \tag{6}$$

$$V_3 = 3[m^2] - 2[m^3], \tag{7}$$

$$V_4 = (4[m] - [m^4])/3, \tag{8}$$

$$V_5 = (3[m] - [m^3])/2, \tag{9}$$

$$V_6 = 2[m] - [m^2], \tag{10}$$

with

$$[m^n] = \ln \frac{\partial \langle m^n \rangle}{\partial T}, \tag{11}$$

which all show the same scaling behavior at the phase transition,

$$V_l \propto L^{1/\nu}. \tag{12}$$

Here, ν is the critical exponent of the correlation length ξ. Now we perform linear fits of the V_l as functions of the system size L in a double-logarithmic plot and compare the slopes obtained, while varying the temperature at which the V_l are evaluated. Since only at the critical temperature T_c all fits have the same slope $1/\nu$, we plot the slope from the fitting procedure for the quantities V_l as a function of l and change the temperature until the points lie on a horizontal line (see Fig. 4). The corresponding temperature is then an estimate for the critical temperature, and the common slope gives the critical exponent ν.

In our case, the obtained values of T_c for $r_c=2.5$ and $r_c=4$ were 7.729 and 11.3175, those of $1/\nu$ were 1.5617 and 1.5795, which correspond to $\nu=0.64$ and $\nu=0.633$. Interestingly, the resulting values of ν are close to the lattice value of the 3D Ising model, $\nu_l=0.6301$ [30], whereas we would rather expect the Fisher-renormalized value $\nu' = \frac{\nu_l}{1-\alpha_l} = 0.708$, where $\alpha_l=0.11$ is the lattice value of the heat capacity exponent.

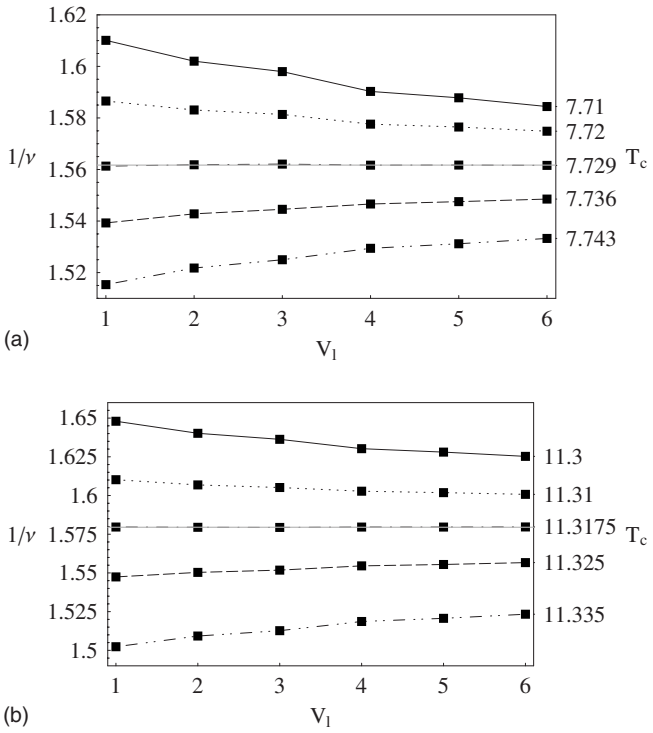

FIG. 4. Quantity dependence of scanning results for the functions V_l for the Ising fluids with $\lambda=1$ and a cutoff radius of $r_c=2.5$ (a) and $r_c=4$ (b). The values of $1/\nu$ for $T_c=7.729$ and $T_c=11.3175$, respectively, shown by the horizontal lines, are 1.5617 ($\nu=0.64$) and 1.5795 ($\nu=0.633$), whereas the values obtained from FSS are $\nu=0.64$ and $\nu=0.629$.

Next, we extrapolated the peak temperatures of the quantities $\partial \ln\langle m^2\rangle/\partial K$, $\partial \ln\langle |m| \rangle/\partial K$, and χ, with $K=\epsilon/k_BT$, as functions of the system size, using the expression (cf. [29])

$$T_{\text{peak}}(L) = T_c + AL^{-1/\nu'}(1 + BL^{-\omega}), \tag{13}$$

where ν' is again the Fisher-renormalized lattice value of the 3D Ising model, A and B are fitting parameters, and ω is some correction exponent. We expect two kinds of corrections to scaling to appear: on the one hand, the usual Wegner corrections [46], with an exponent proportional to $\Delta \approx 0.5$, and on the other hand the so-called Fisher corrections to scaling [47,48], proportional to $|\alpha|$, which should decay much slower with approaching the asymptotic region since $\alpha=0.11$ for the 3D Ising model. The latter are caused by the same constraint-induced temperature rescaling which is also responsible for the Fisher renormalization of the critical exponents. In (13), only a single correction term with one exponent has been assumed since including more than one term leaves too few degrees of freedom in the fit.

At $L=\infty$ the three curves should meet at a common T_c. This method is known as the shifting technique because of the shift of the maxima in finite systems with respect to the critical temperature of the infinite system. We have also tried linear fits without the correction term in (13), but in that case the lines cross already far from the limit $L \to \infty$, indicating that corrections to scaling cannot be neglected.

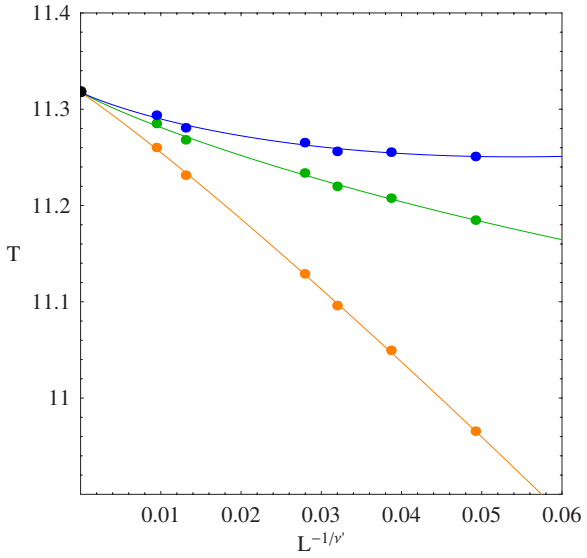

FIG. 5. (Color online) Size dependence of the peak locations of the quantities (top to bottom) $\partial \ln m^2/\partial K$, $\partial \ln |m|/\partial K$, and χ, with $K=\epsilon/k_BT$, for the Ising fluid with $\lambda=1$ and a cutoff radius of $r_c=4$. The MC data corresponding to the particle numbers $N=300,500,750,1000,5000,10\,000$ have been fitted using expression (13). The mean critical temperature of the fits is $T_c=11.3174(1)$, marked by a black dot at $L=\infty$.

We first applied the nonlinear fit (13) to the data obtained for the Ising fluid with $r_c=4$, using only the four largest particle numbers ($N=750$, 1000, 5000, and 10 000) for the fit. With the correction exponents 0.14, 0.28, and 0.23 for $\partial \ln\langle m^2\rangle/\partial K$, $\partial \ln\langle |m|\rangle/\partial K$, and χ, respectively, the curves intersect at $L=\infty$ at an average critical temperature of $T_c=11.3293(1)$. This value, however, does not compare well with the values obtained from the cumulant crossing [$T_c=11.3189(76)$] and the scanning technique ($T_c=11.3175$). A considerably better result is achieved when taking into account also the data from the two smaller system sizes, $N=300$ and $N=500$. In that case, the curves coincide at $T_c=11.3174(1)$ (see Fig. 5), and the correction exponents are 0.52, 0.31, and 0.47. Concerning the size of the corrections to scaling we can say that the term $BL^{-\omega}$ in (13) can be neglected if it is smaller than 0.5. Taking into account that the absolute value of B was found to lie roughly between 1 and 2, we obtain that for the case of the smallest correction exponent 0.31 this condition is fulfilled if $N \gtrsim 30\,000$. Since the largest system sizes we could study with our computational resources was 10 000, it is clear why we must take into account the correction term.

So far we have assumed that the exponent in (13) is the Fisher-renormalized ν'. If we repeat the fitting procedure using the unrenormalized exponent ν_l instead, again with all system sizes included, the agreement of T_c with the other two results gets worse again, although the obtained value [$T_c=11.3141(1)$] is still within the error bars of the cumulant crossing result.

A similar investigation using the shifting technique for a cutoff radius $r_c=2.5$ yielded a critical temperature of $T_c=7.7213(1)$.

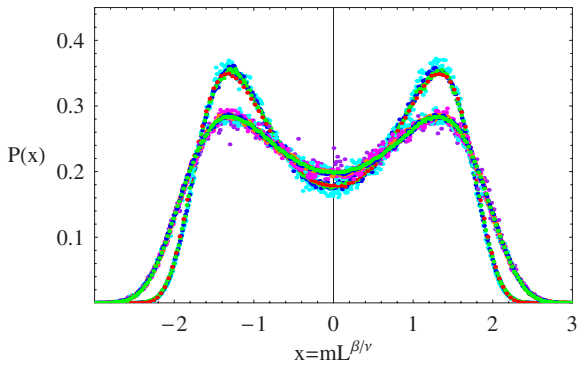

FIG. 6. (Color online) Critical probability distribution function $P(x)$, where $x=mL^{\beta/\nu}$ is the scaled magnetization, for Ising fluids with $\lambda=1$ and $r_c=2.5$ and $r_c=4$. The value of β/ν is 0.54 for $r_c=2.5$ and 0.61 for $r_c=4$. The individual data correspond to the system sizes $N=108$, 300, 500, 750, 1000, 5000, and 10 000.

D. Scaling and critical exponents

When scaling the magnetization with a factor $L^{\beta/\nu}$, β being the critical exponent of the magnetization, the normalized distribution functions P ($x\equiv mL^{\beta/\nu}$) at the critical temperature should collapse for all system sizes. This is demonstrated in Fig. 6 for Ising fluids with $r_c=2.5$ and $r_c=4$. We see that the scaled distributions belonging to different system sizes but the same r_c coincide, whereas those corresponding to different r_c do not. The different shapes of the scaling functions, reflecting the different values of the critical Binder cumulant, are clearly visible.

The value of β/ν used in the scaling was derived from the slope of the critical magnetization value $m_c\equiv\langle |m|\rangle(T_c)$ as a function of the linear system size L in a double-logarithmic plot, according to the FSS relation [15]

$$m_c \propto L^{-\beta/\nu}. \tag{14}$$

Figure 7 shows straight-line fits $\ln m_c = c-(\beta/\nu)\ln L$, with c being some constant, for Ising fluids with different cutoff radii r_c. From the plot, a continuous change in the slope of the lines is clearly visible. The statistical errors ϵ of the values of $\ln m_c$ used in the chi-square fitting procedure were obtained from the standard deviation σ of the averaged result of n simulations performed in parallel as

$$\epsilon = \frac{\sigma}{n}. \tag{15}$$

Q values of the fits (see, for example, Ref. [49] for a definition) lay between 0.6 and 0.9. In Fig. 8(a), β/ν is shown as a function of the cutoff radius r_c. A distinct dependence on r_c can be seen, with β/ν being 0.505(5) for $r_c=2$ and reaching a value of 0.633(9) for $r_c=5$, whereas the lattice Ising value is 0.519(2) [30].

Next, we looked at the value of γ/ν, obtained from the FSS relation [15]

$$\chi_{\max} \propto L^{\gamma/\nu}, \tag{16}$$

where χ is the susceptibility

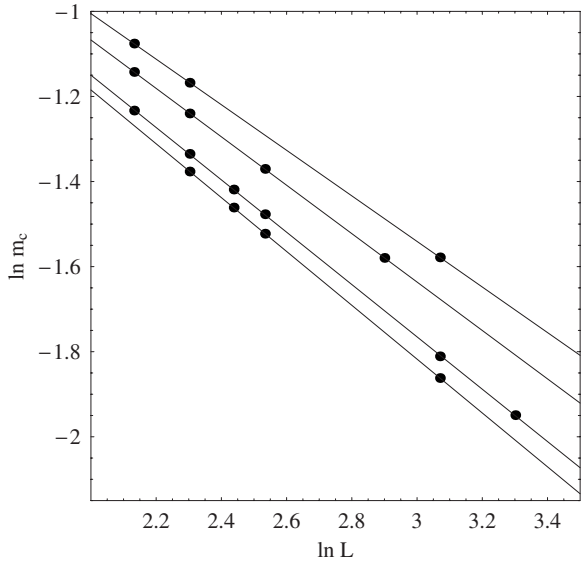

FIG. 7. Magnetization at the critical temperature m_c as a function of the system size L on a log-log scale for the Ising fluid with $\lambda=1$ and various cutoff radii $r_c=2.5,3,4,5$ (top to bottom). The lines correspond to straight-line fits to the data. The changing slopes reflect the different values of β/ν.

$$\chi = \frac{V}{k_B T}(\langle m^2\rangle - \langle |m|\rangle^2), \tag{17}$$

and $\chi_{\max}$ the maximum of χ as a function of temperature. Figure 9 again shows the straight-line fits $\ln \chi_{\max} = c + (\gamma/\nu)\ln L$ for Ising fluids with different cutoff radii r_c. Once more, the slope changes significantly with r_c, and γ/ν shows a similar behavior as β/ν [only decreasing instead of increasing, see Fig. 8(b)]. The goodness Q of the fits was in the region 0.4–0.9.

On the other hand, for the critical exponent ν itself no significant r_c dependence was observed [Fig. 8(c)], its value staying close to that of the 3D Ising universality class, $\nu=0.6301$, in the whole r_c range. Estimates for $1/\nu$ were obtained as mean values of the three slopes derived from the FSS relations [29]

$$\left(\frac{\partial \ln\langle |m|\rangle}{\partial T}\right)_{\min} \sim L^{1/\nu}, \tag{18}$$

$$\left(\frac{\partial \ln\langle m^2\rangle}{\partial T}\right)_{\min} \sim L^{1/\nu}, \tag{19}$$

and

$$\left(\frac{\partial U}{\partial T}\right)_{\min} \sim L^{1/\nu}. \tag{20}$$

The derivatives were calculated from the histogram $H(m,E)$ as cross correlations with the energy E, as described in [29],

$$\frac{\partial}{\partial K}\langle m^n\rangle = \langle m^n\rangle\langle E\rangle - \langle m^n E\rangle, \tag{21}$$

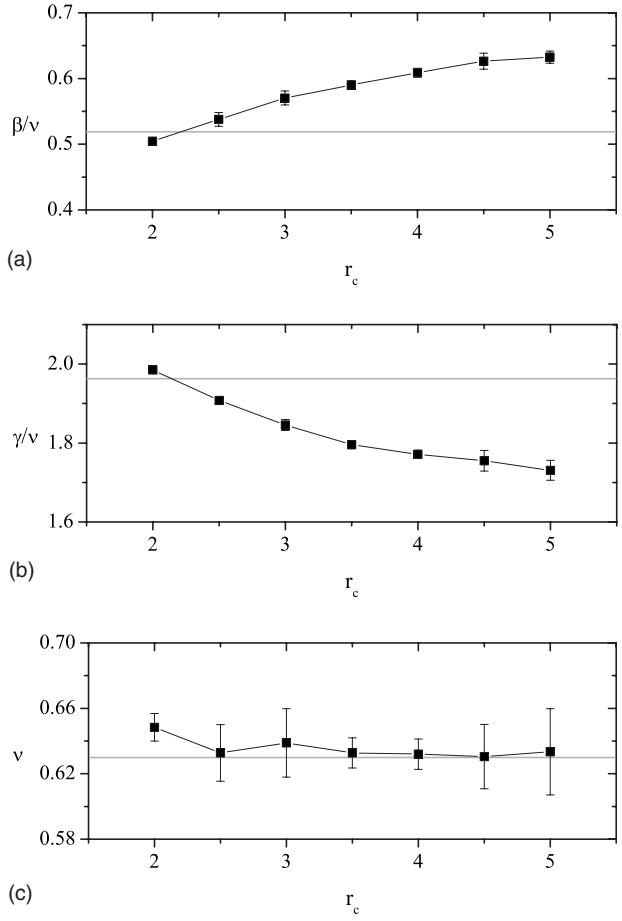

FIG. 8. Critical exponent ratios β/ν (a), γ/ν (b), and critical exponent ν (c) of the Ising fluid with $\lambda=1$ as a function of the cutoff radius r_c. The horizontal lines indicate the corresponding values for the 3D lattice Ising model ($\beta/\nu=0.519$, $\gamma/\nu=1.963$, $\nu=0.6301$ [30]).

$$\frac{\partial}{\partial K}\ln\langle m^n\rangle = \frac{1}{\langle m^n\rangle}\frac{\partial}{\partial K}\langle m^n\rangle = \langle E\rangle - \frac{\langle m^n E\rangle}{\langle m^n\rangle}. \tag{22}$$

The subscript "min" always denotes the minimum with respect to temperature. These minima were found by calculating the second derivatives with respect to K, for example,

$$\frac{\partial^2\langle |m|\rangle}{\partial K^2} = \langle |m|E^2\rangle - \langle |m|\rangle\langle E^2\rangle + 2\langle E\rangle\frac{\partial\langle |m|\rangle}{\partial K}, \tag{23}$$

and finding the roots of these functions.

Straight-line fits to Eq. (18) are shown in Fig. 10, demonstrating that in this case no apparent change in the slope with varying r_c occurs. However, a large uncertainty is connected with the obtained values of ν [see Fig. 8(c)], mostly due to the third relation (20) including the Binder cumulant, which is afflicted with a rather high statistical error. Also, the first two values were usually lying rather close together, while the third one differed considerably from the others. Still, the Q values of the fits were at least 0.4 in all cases.

In Tables I and II, both for $r_c=2.5$ and $r_c=4$, the results for the different techniques are summarized, including criti-

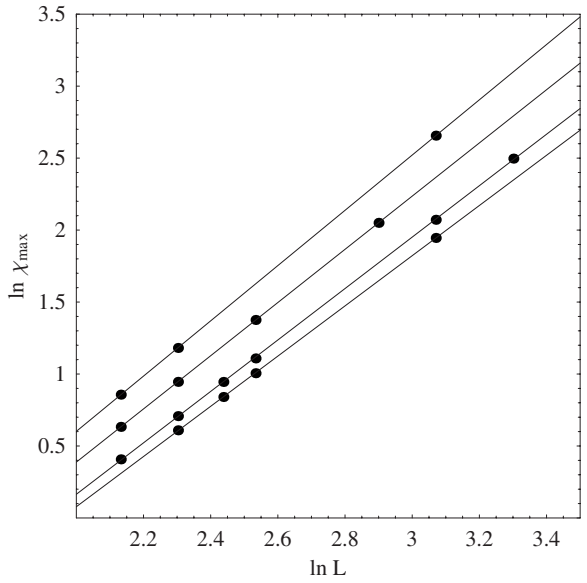

FIG. 9. Maximum of the susceptibility χ_{max} as a function of the system size L on a log-log scale for the Ising fluid with $\lambda=1$ and various cutoff radii $r_c=2.5,3,4,5$ (top to bottom). The lines correspond to straight-line fits to the data. The changing slopes reflect the different values of γ/ν.

cal temperatures and critical exponents. The corresponding values for the three-dimensional lattice Ising model are also included.

We also tried to obtain data on the specific heat C, where

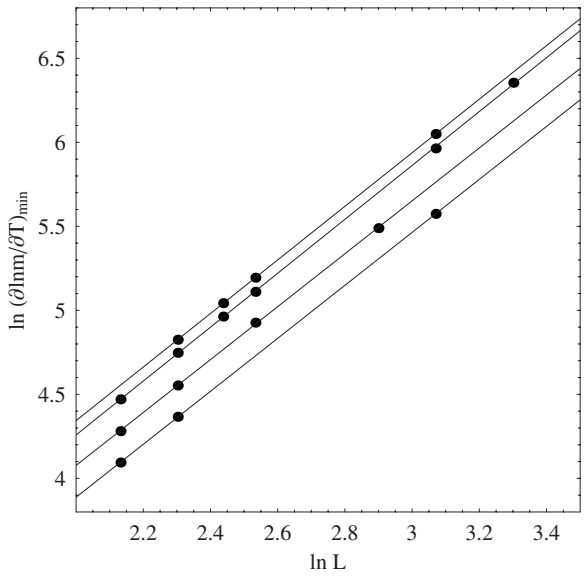

FIG. 10. Minimum of the logarithmic derivative of the magnetization $\left(\frac{\partial \ln\langle|m|\rangle}{\partial T}\right)_{min}$ as a function of the system size L on a log-log scale for the Ising fluid with $\lambda=1$ and various cutoff radii $r_c=2.5,3,4,5$ (bottom to top). The lines correspond to straight-line fits to the data. The slopes $1/\nu$ do not change significantly.

TABLE I. Results for critical temperature and critical exponents from the scanning technique (column V_i), the cumulant crossing technique (column U) and the shifting technique (column FSS), for the Ising fluid with $\lambda=1$ and a cutoff radius of $r_c=4$. For the critical temperature in column FSS, the T_c extrapolation with all six system sizes and the Fisher-renormalized ν' (Fig. 5) was used. The last row gives the value of β/ν depending on the value of T_c used in the fitting of $m_c(L)$.

	V_i	U	FSS	Lattice
T_c	11.3175	11.3189(76)	11.3174(1)	4.51152(2)
$1/\nu$	1.58		1.58(2)	1.587(2)
γ/ν			1.77(1)	1.963(3)
β/ν	0.609(7)	0.612(7)	0.609(7)	0.519(2)

$$C=\frac{1}{V(k_BT)^2}(\langle E^2\rangle-\langle|E|\rangle^2), \tag{24}$$

and the corresponding critical exponent α from the simulations. However, it turns out that the peaks of $C(T)$ in the finite systems lie too far away from the critical temperature T_c of the infinite system and thus from the simulation temperatures, to get reliable results from the histogram reweighting technique. In some cases, one cannot even see a peak at all. Figure 11 shows resulting curves $C(T)$ for $r_c=4$ and system sizes $N=300$, 1000, and 5000 (the curves for the other system sizes show no peak in this case). As the increasing height of the peak indicates, the sign of α seems to be positive, which would contradict a Fisher renormalization. Linear interpolation in a double-logarithmic plot yields 0.25(9) for the slope α/ν, which corresponds to a highly inaccurate value of $\alpha=0.16(6)$.

As we already pointed out in Sec. II C, the small correction exponents prevent us from reaching the asymptotic region with the available computer power. Thus, the values of the critical exponents we observe can be explained as effective exponents. A way to obtain more information about the asymptotic exponents was introduced by Orkoulas *et al.* [50]. By performing simulations away from the critical region, the bulk behavior of the effective exponents β_{eff} and γ_{eff} as functions of temperature can be investigated and extrapolated towards T_c to estimate the asymptotic exponents by means of theoretical series expansion data. This is made possible because of the sharp departure from the limiting behavior when approaching the critical temperature. This extrapolation allowed them to determine the universality class

TABLE II. The same as in Table I for the Ising fluid with $\lambda=1$ and a cutoff radius of $r_c=2.5$.

	V_i	U	FSS	Lattice
T_c	7.729	7.7234(58)	7.7213(1)	4.51152(2)
$1/\nu$	1.56		1.57(4)	1.587(2)
γ/ν			1.907(6)	1.963(3)
β/ν	0.541(7)	0.537(7)	0.528(7)	0.519(2)

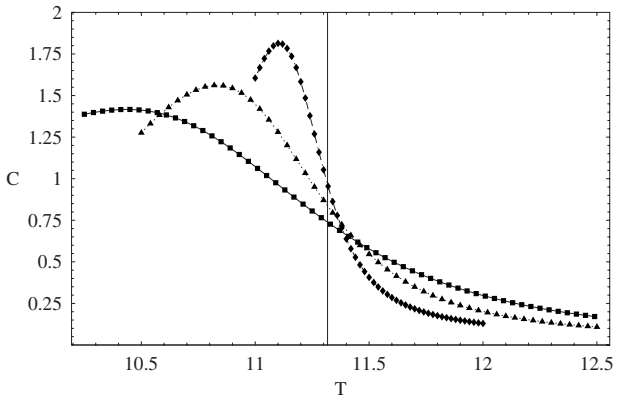

FIG. 11. Specific heat C as a function of temperature for the Ising fluid with $\lambda=1$ and a cutoff radius $r_c=4$, and system sizes $N=300$ (squares), 1000 (triangles), and 5000 (diamonds). The increasing peak heights indicate a positive value of α. The vertical line marks the critical temperature of the infinite system ($T_c=11.3175$).

of the three-dimensional Ising model with different numbers of nearest-neighbor couplings by ruling out exponents belonging to other universality classes (self-avoiding walk, XY model). Later, the same authors used this method also for the hard-core square-well fluid [51], confirming its universality class to be of the Ising type. We have applied the same technique to the Ising fluids with $r_c=2.5$ and $r_c=4$. We calculated the effective exponent $\gamma^+_{\text{eff}}(T)$ as

$$\gamma^+_{\text{eff}}(T) = -\frac{\partial \ln \chi}{\partial \ln|t|},$$

where

$$t = 1 - T_c/T,$$

for different system sizes and have plotted the results in Fig. 12 as functions of $(T-T_c)/T$. Since there is no series expansion data for Ising fluid systems available, we cannot make an exact extrapolation, but judging from the curves for $r_c=2.5$, whose peaks lie above the value of γ_l, the lattice value of the 3D Ising model, the results point towards the Fisher-renormalized value of $\gamma'=1.39$. It is also interesting to note that the curve for the Ising fluid with $r_c=4$ and $N=5000$ seems to show a slightly nonmonotonic behavior, going to a minimum near $t=0.15$ before approaching the $N=1000$ curve again. This could be an indication of the interplay between two types of corrections to scaling with different signs, on the one hand, the Wegner correction which is only important further away from the critical temperature, and on the other hand, the Fisher-type correction which becomes dominant for smaller values of t.

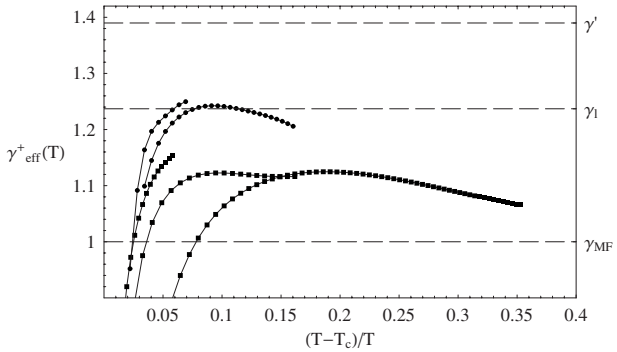

FIG. 12. Effective susceptibility exponent $\gamma^+_{\text{eff}}(T)$ for $T>T_c$ for the Ising fluid with $\lambda=1$, $r_c=4$ (squares) and system sizes $N=1000$, 5000, and 10 000 (right to left), and for the Ising fluid with $\lambda=1$, $r_c=2.5$ (circles) and $N=5000$ and 10 000 (right to left). Indicated as horizontal lines are the value of γ in the mean-field theory ($\gamma_{\text{MF}}=1$), the value of the 3D Ising lattice model ($\gamma_l=1.237$ [30]) and the Fisher-renormalized lattice value $\left(\gamma'=\frac{\gamma_l}{1-\alpha_l}=1.39\right)$.

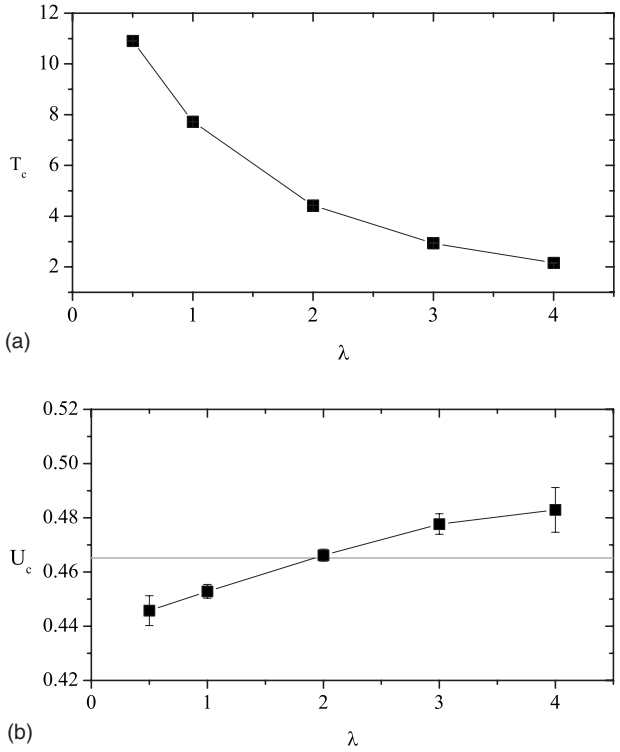

FIG. 13. Critical temperature T_c (a) and critical Binder cumulant U_c (b) of the Ising fluid with cutoff radius $r_c=2.5$ as a function of the screening parameter λ. The horizontal line indicates the value of U_c for the lattice Ising model [30].

E. Varying λ

In another set of simulations we have also studied the influence of the screening parameter λ in the Yukawa potential (2) on the critical quantities at the ferromagnetic phase transition. At a fixed cutoff radius $r_c=2.5$ we varied the value of λ between 0.5 and 4 and performed the same kinds of simulations as described in the preceding section. While the dependence of the critical temperature T_c on the interaction potential parameter [Fig. 13(a)] is as expected, the value of the fourth-order cumulant at T_c, U_c, shows again an unexpected nonuniversal behavior, rising from 0.446(5) to 0.483(8) with increasing λ [Fig. 13(b)]. With rising λ, however, the corrections to scaling now also increase, reflecting

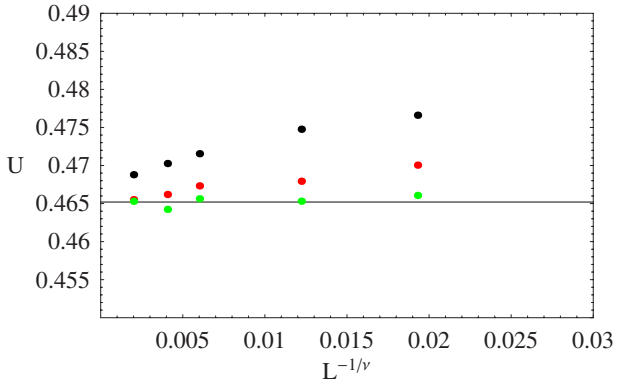

FIG. 14. (Color online) Dependence of the Binder cumulant U of the 3D Ising lattice at T_c on the system size L. The points correspond to the NN, NN+NNN, and NN+NNN+3NN systems (top to bottom). The horizontal line indicates the known value of U_c =0.4652 for the lattice Ising model [30].

the decrease in the effective range of the Yukawa function with larger screening parameter.

III. ISING LATTICE

We have also performed additional simulations on a three-dimensional Ising lattice. Our motivation is to compare the effect of the interaction range in a system where Fisher renormalization is expected (Ising fluid) with that in a system without a thermodynamic constraint, where no such renormalization should occur (Ising lattice). Apart from the different values of the critical exponents, Fisher corrections to scaling are also absent in the latter system, making it easier to reach the asymptotic region.

In order to examine the influence of the range of the exchange interaction we have successively included nearest-neighbor (NN), next-nearest-neighbor (NNN), and third-nearest-neighbor (3NN) couplings, respectively. The strengths of the particular interactions were chosen equal to the strength of the Yukawa interaction $J(r)$ (2) used in the Ising fluid at the corresponding lattice distances, assuming a number density of $N/V=0.5\sigma^{-3}$. For such a lattice, the lattice constant is $a=\sqrt[3]{2}\approx 1.26$ (in units of σ), the distance of next-nearest neighbors is $a_{\mathrm{NNN}}=\sqrt{2}a\approx 1.78$, and that of the third-nearest neighbors $a_{\mathrm{3NN}}=\sqrt{3}a\approx 2.18$. The corresponding coupling constants are $J_{\mathrm{NN}}=J(a)=0.612$, $J_{\mathrm{NNN}}=J(a_{\mathrm{NNN}})=0.2568$, and $J_{\mathrm{3NN}}=J(a_{\mathrm{3NN}})=0.1405$, and the Hamiltonian is given by

$$\mathcal{H}=-J_{\mathrm{NN}}\sum_{\langle ij\rangle}s_is_j-J_{\mathrm{NNN}}\sum_{\langle\langle ij\rangle\rangle}s_is_j-J_{\mathrm{3NN}}\sum_{\langle\langle\langle ij\rangle\rangle\rangle}s_is_j, \quad (25)$$

where the sums go over nearest, next-nearest, and third-nearest, neighbors, respectively. As the reduced temperature we used $T^*=k_BT/J_{\mathrm{NN}}$. Simulations were performed for different lattice sizes L, ranging from $L=6$ to $L=50$, with particle numbers $N=L^3$. The simulation runs consisted of 10^7 MC cycles, each comprising one Wolff cluster move.

Figure 14 shows the finite-size dependence of the value of $U_c=U(T_c)$ for the three systems we considered, namely one with pure NN couplings, one with NN- plus-NNN couplings, and one with all three couplings turned on (for the NN system such a plot was shown in Fig. 7 of Ref. [29]). The corresponding critical temperatures are $T_c^{\mathrm{NN}}=4.5115$, $T_c^{\mathrm{NNN}}=9.2806$, and $T_c^{\mathrm{3NN}}=11.123$. The graph shows clearly that in every case U_c tends with larger system size to the value that is usually connected with the Ising universality class, which is $U_c=0.4652$ [30]. As expected, no dependence on the interaction range is found. There is however, a clear decrease of the finite-size dependence with increasing number of neighbors included in the Hamiltonian (this was already mentioned in [30]). While for the pure NN case, the deviations due to the finite system size are quite large ($U_c\approx 0.477$ at $L=12$), for the NN+NNN+3NN system the values of U_c are close to the infinite-size limit already for rather small systems ($U_c\approx 0.466$ at $L=12$). This can also be seen in Fig. 15, where the cumulant intersection regions for the NN and NN

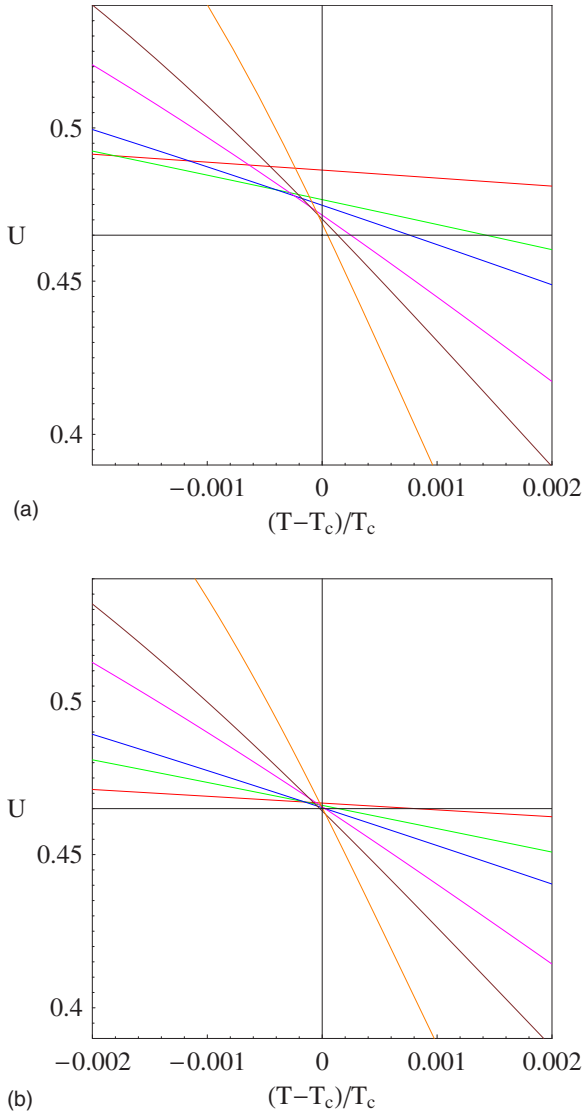

FIG. 15. (Color online) Binder cumulant $U_L(T)$ of the 3D Ising lattice for different sizes ($L=6,\ldots,50$) for the NN (a) and the NN +NNN+3NN system (b). The horizontal and vertical lines indicate the locations of U_c and T_c, respectively.

+NNN+3NN systems are displayed. The intersection points of the separate curves obviously lie much closer together in the latter case. It is also interesting to compare with Fig. 1, showing the corresponding plots for the Ising fluids with $r_c=2.5$ and $r_c=4$, which exhibit a similar though less pronounced trend. Since the mean number of neighbors lying within the cutoff radius r_c around a particle in an Ising fluid simulation is roughly equal to the number of neighbors closer than the distance r_c in a lattice with the same density, we expect the errors in the value of U_c due to corrections to scaling to be of about the same order of magnitude as in the corresponding lattice simulations. For large $r_c \gtrsim 3$, the error can be expected to be smaller than 0.01, which is consistent with our error bars.

IV. CONCLUSION

We have studied the ferromagnetic order-disorder transition in hard-core Ising fluids with Yukawa exchange interaction truncated at various cutoff radii r_c, and also with different inverse screening lengths λ. We performed Monte Carlo simulations in the canonical ensemble, analyzing the obtained data via histogram reweighting and different finite-size scaling techniques. In the case of $r_c=2.5$ and $\lambda=1$, our results for the critical Binder cumulant and critical exponent ratios agree with those of Nijmeijer, Parola, and Reatto [8], however for other values of the parameters we find significant deviations from these results. Keeping $\lambda=1$ constant and increasing r_c, the critical Binder cumulant U_c as well as γ/ν decrease far below the corresponding values of the lattice Ising model, while β/ν increases above and ν itself stays close to its lattice counterpart. Also with assuming Fisher renormalization of the exponents, which is expected for Ising fluids at constant density due to $\alpha>0$, these results cannot be explained satisfyingly.

A closer inspection of the corrections to finite-size scaling in the shifting technique reveals a rather small transient that prevents reaching the asymptotic critical region even with the largest system sizes that can be studied with our computers. A rough estimate shows that particle numbers of at least 30 000 would be necessary. Therefore, the exponents we have measured are merely effective ones, like those in [9] for the case of the Heisenberg fluid. For the effective critical exponent γ_{eff} we have performed a detailed investigation of the bulk behavior away from T_c which allows us to estimate the asymptotic value. From the resulting curves, at least for $r_c=2.5$, we see a tendency towards a Fisher-renormalized value of γ.

The question whether the observed values of U_c are also just effective ones or whether they really depend on the details of the interaction potential, remains open until simulations with higher particle numbers are performed. With the system sizes we have used, no noticeable trend was observed that would indicate a crossover to the lattice value of U_c. Simulations of the simple cubic 3D Ising model with different numbers of couplings (nearest neighbor, next-nearest neighbor, and third-nearest neighbor) included in the Hamiltonian, their strengths chosen according to the Yukawa interaction in the Ising fluid, show no sign of a change in the critical Binder cumulant. Only the additional translational degrees of freedom in the liquid system seem to cause the nonuniversal results obtained.

ACKNOWLEDGMENTS

The authors acknowledge support by the Fonds zur Förderung der Wissenschaftlichen Forschung under Contract No. P18592-TPH. The authors also thank Walter Selke for his comments on an early draft of this paper.

[1] M. E. Fisher, Phys. Rev. **176**, 257 (1968).
[2] B. Widom, J. Chem. Phys. **46**, 3324 (1967).
[3] G. Neece, J. Chem. Phys. **47**, 4112 (1967).
[4] R. K. Clark, J. Chem. Phys. **48**, 741 (1968).
[5] M. Blume, Phys. Rev. **141**, 517 (1966).
[6] H. W. Capel, Physica (Amsterdam) **32**, 966 (1966).
[7] M. Blume, V. J. Emery, and R. B. Griffiths, Phys. Rev. A **4**, 1071 (1971).
[8] M. J. P. Nijmeijer, A. Parola, and L. Reatto, Phys. Rev. E **57**, 465 (1998).
[9] I. M. Mryglod, I. P. Omelyan, and R. Folk, Phys. Rev. Lett. **86**, 3156 (2001).
[10] M. J. P. Nijmeijer and J. J. Weis, Phys. Rev. E **53**, 591 (1996).
[11] M. J. P. Nijmeijer and J. J. Weis, Phys. Rev. Lett. **75**, 2887 (1995).
[12] E. Lomba, C. Martín, and N. G. Almarza, Eur. Phys. J. B **34**, 473 (2003).
[13] E. Lomba, C. Martín, and N. G. Almarza, Mol. Phys. **101**, 1667 (2003).
[14] E. Lomba and C. Martín, Condens. Matter Phys. **6**, 551 (2003).
[15] K. Binder, Z. Phys. B: Condens. Matter **43**, 119 (1981).
[16] X. S. Chen and V. Dohm, Phys. Rev. E **70**, 056136 (2004).
[17] X. S. Chen and V. Dohm, Phys. Rev. E **71**, 059901(E) (2005).
[18] W. Selke, Eur. Phys. J. B **51**, 223 (2006).
[19] G. Kamieniarz and H. W. J. Blöte, J. Phys. A **26**, 201 (1993).
[20] W. Selke and L. N. Shchur, J. Phys. A **38**, L739 (2005).
[21] T. W. Burkhardt and B. Derrida, Phys. Rev. B **32**, 7273 (1985).
[22] A. Drzewinski and J. Wojtkiewicz, Phys. Rev. E **62**, 4397 (2000).
[23] R. Hilfer, B. Biswal, H. G. Mattutis, and W. Janke, Phys. Rev. E **68**, 046123 (2003).
[24] W. Janke, M. Katoot, and R. Villanova, Phys. Rev. B **49**, 9644 (1994).
[25] W. Rzysko, A. Patrykiejew, and K. Binder, Phys. Rev. B **72**, 165416 (1994).
[26] C. Holm, W. Janke, T. Matsui, and K. Sakakibara, Physica A **246**, 633 (1997).
[27] G. Schmid, S. Todo, M. Troyer, and A. Dorneich, Phys. Rev. Lett. **88**, 167208 (2002).
[28] M. Holtschneider, W. Selke, and R. Leidl, Phys. Rev. B **72**, 064443 (2005).

[29] A. M. Ferrenberg and D. P. Landau, Phys. Rev. B **44**, 5081 (1991).
[30] H. W. J. Blöte, E. Luijten, and J. R. Heringa, J. Phys. A **28**, 6289 (1995).
[31] M. Schulte and C. Drope, Int. J. Mod. Phys. C **16**, 1217 (2005).
[32] M. A. Sumour, D. Stauffer, M. M. Shabat, and A. H. El-Astal, Physica A **368**, 96 (2006).
[33] P. C. Hemmer and D. Imbro, Phys. Rev. A **16**, 380 (1977).
[34] N. E. Frankel and C. J. Thompson, J. Phys. C **8**, 3194 (1975).
[35] F. Schinagl, H. Iro, and R. Folk, Eur. Phys. J. B **8**, 113 (1999).
[36] W. Fenz, R. Folk, I. M. Mryglod, and I. P. Omelyan, Phys. Rev. E **68**, 061510 (2003).
[37] W. Fenz and R. Folk, Condens. Matter Phys. **6**, 675 (2003).
[38] I. P. Omelyan, W. Fenz, R. Folk, and I. M. Mryglod, Eur. Phys. J. B **51**, 101 (2006).
[39] I. P. Omelyan, I. M. Mryglod, R. Folk, and W. Fenz, Phys. Rev. E **69**, 061506 (2004).
[40] A. Parola and L. Reatto, Adv. Phys. **44**, 211 (1995).
[41] U. Wolff, Phys. Rev. Lett. **62**, 361 (1989).
[42] D. Frenkel and B. Smit, *Understanding Molecular Simulation* (Academic, New York, 2002).
[43] A. M. Ferrenberg and R. H. Swendsen, Phys. Rev. Lett. **61**, 2635 (1988).
[44] A. M. Ferrenberg and R. H. Swendsen, Phys. Rev. Lett. **63**, 1195 (1989).
[45] K. Chen, A. M. Ferrenberg, and D. P. Landau, Phys. Rev. B **48**, 3249 (1993).
[46] F. Wegner, Phys. Rev. B **5**, 4529 (1972).
[47] I. M. Mryglod and R. Folk, Physica A **294**, 351 (2001).
[48] M. Krech, *Computer Simulation Studies in Condensed Matter Physics XII* (Springer, Berlin, 1999).
[49] W. H. Press, B. P. Flannery, S. A. Teukolsky, and W. T. Vetterling, *Numerical Recipes in C*, 2nd ed. (Cambridge University Press, Cambridge, 1992), Chap. 15.
[50] G. Orkoulas, A. Z. Panagiotopoulos, and M. E. Fisher, Phys. Rev. E **61**, 5930 (2000).
[51] G. Orkoulas, M. E. Fisher, and A. Z. Panagiotopoulos, Phys. Rev. E **63**, 051507 (2001).